Soliton-induced optical absorption of halogen-bridged mixed-valence binuclear metal complexes

Jun Ohara and Shoji Yamamoto

Division of Physics, Hokkaido University, Sapporo 060-0810, Japan

Employing the one-dimensional single-band extended Peierls-Hubbard model, we investigate optical conductivity for solitonic excitations in halogen-bridged binuclear metal (MMX) complexes. Photoinduced soliton absorption spectra for MMX chains possibly split into two bands, forming a striking contrast to those for conventional mononuclear metal (MX) analogs, due to the broken electron-hole symmetry combined with relevant Coulomb and/or electron-phonon interactions.

I. INTRODUCTION

Halogen (X)-bridged mixed-valence metal (M) complexes [1,2] such as $[Pt(en)_2X](ClO_4)_2$ ($X = Cl, Br, I$; en = ethylenediamine = $C_2H_8N_2$), which are referred to as MX chains, have been playing a prominent role in understanding the electronic properties of one-dimensional Peierls-Hubbard systems. The competing electron-electron and electron-phonon interactions yield various ground states [3,4], which can be tuned by chemical substitution [5] and pressure [6]. Solitonic excitations inherent in charge-density-wave (CDW) ground states stimulate further interest in MX complexes. In this context, we may be reminded of polyacetylene, the trans isomer of which exhibits topological solitons [7,8]. Several authors [9–11] had an idea of similar defect states existing in MX chains. Photogenerated solitons [12,13] were indeed observed in the PtX compounds.

In recent years, binuclear metal analogs of MX complexes, which are referred to as MMX chains, have attracted further interest exhibiting a wider variety of ground states [14,15], successive thermal phase transitions [16,17], photo- and pressure-induced phase transitions [18–20], and incomparably larger room-temperature conductivity [21]. In such circumstances, soliton solutions of an MMX Hamiltonian of the Su-Schrieffer-Heeger type [7] have recently been investigated both analytically and numerically [22]. The direct $M-M$ overlap contributes to the reduction of the effective on-site Coulomb repulsion and therefore electrons can be more itinerant in MMX chains. Hence we take more and more interest in solitons as charge or spin carriers.

The ground-state properties of MMX complexes were well revealed by means of X-ray diffraction [23], nuclear magnetic resonance [24], and the Raman and Mössbauer spectroscopy [16], while very little [25,26] is known about their excitation mechanism. *Photoinduced* absorption spectra, which served as prominent probes for nonlinear excitations in MX complexes [12,13], have, to our knowledge, not yet measured on MMX complexes probably due to the lack of a guiding theory. Thus motivated, we study optical conductivity for MMX solitons with particular emphasis on a contrast between topical MMX and conventional MX complexes. Photoexcited MMX chains may yield distinct spectral shapes due to the definite breakdown of the electron-hole symmetry.

II. MODEL HAMILTONIANS AND THEIR GROUND-STATE PROPERTIES

We describe MX and MMX chains by the one-dimensional $\frac{1}{2}$- and $\frac{3}{4}$-filled single-band Peierls-Hubbard Hamiltonians

$$\mathcal{H}_{MX} = h_{MXM}^{(1,1)} + h_M^{(1,1)} + h_{MX}, \tag{1a}$$

$$\mathcal{H}_{MMX} = h_{MM}^{(1,2)} + h_{MXM}^{(1,2)} + h_M^{(1,2)} + h_{MX}, \tag{1b}$$

respectively, where

$$h_{MM}^{(\mu,\nu)} = -t_{MM} \sum_{n,s}(a_{\mu:n,s}^\dagger a_{\nu:n,s} + a_{\nu:n,s}^\dagger a_{\mu:n,s})$$
$$+ V_{MM} \sum_{n,s,s'} n_{\mu:n,s} n_{\nu:n,s'}, \tag{2}$$

$$h_{MXM}^{(\mu,\nu)} = -\sum_{n,s}[t_{MXM} - \alpha(l_{n+1}^{(-)} + l_n^{(+)})](a_{\mu:n+1,s}^\dagger a_{\nu:n,s}$$
$$+ a_{\nu:n,s}^\dagger a_{\mu:n+1,s}) + V_{MXM} \sum_{n,s,s'} n_{\mu:n+1,s} n_{\nu:n,s'}, \tag{3}$$

$$h_M^{(\mu,\nu)} = -\beta \sum_{n,s}(l_n^{(-)} n_{\mu:n,s} + l_n^{(+)} n_{\nu:n,s})$$
$$+ \frac{\nu U_M}{2} \sum_n (n_{\mu:n,+} n_{\mu:n,-} + n_{\nu:n,+} n_{\nu:n,-}), \tag{4}$$

$$h_{MX} = \frac{K_{MX}}{2} \sum_n [(l_n^{(-)})^2 + (l_n^{(+)})^2]. \tag{5}$$

Here, $n_{\mu:n,s} = a_{\mu:n,s}^\dagger a_{\mu:n,s}$ with $a_{\mu:n,s}^\dagger$ being the creation operator of an electron with spin $s = \pm\frac{1}{2}$ (up and down) for the M d_{z^2} orbital labeled as $\mu = 1, 2$ in the nth MX or MMX unit, t_{MM} and t_{MXM} describe the intra- and
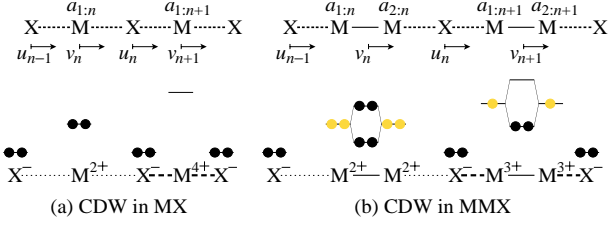
FIG. 1. Schematic representation of CDW ground states observed in MX (a) and MMX (b) complexes.

interunit electron hoppings, respectively, α and β are the site-off-diagonal and site-diagonal electron-lattice coupling constants, respectively, $l_n^{(-)} = v_n - u_{n-1}$ and $l_n^{(+)} = u_n - v_n$ with u_n and v_n being, respectively, the chain-direction displacements of the halogen and metal in the nth unit from their equilibrium position, and K_{MX} is the metal-halogen spring constant. We assume, based on the thus-far reported experimental observations, that every M_2 moiety is not deformed. The notation is further explained in Fig. 1. We set t_{MXM} and K_{MX} both equal to unity in the following.

The existent MMX complexes consist of two families: $R_4[Pt_2(pop)_4X]\cdot nH_2O$ ($X = Cl, Br, I$; $R = Li, K, Cs, \cdots$; pop = diphosphonate = $P_2O_5H_2^{2-}$) and $M_2(dta)_4I$ ($M = Pt, Ni$; dta = dithioacetate = $CH_3CS_2^-$), which are referred to as pop and dta complexes. The pop complexes possess the mixed-valence ground state illustrated in Fig. 1(b) [24,27], while the dta complexes exhibit distinct types of ground states [14–16,28] due to the predominant site-off-diagonal electron-phonon coupling [29] or metal-on-site Coulomb repulsion [30]. Conventional MX complexes structurally resemble MMX complexes of the pop type and have the mixed-valence ground state illustrated in Fig. 1(a) [2], which is symmetrically equivalent to that in Fig. 1(b) [15,31]. Hence we study the pop complexes in our first attempt to compare the photoproducts in MMX and MX chains. While the dta complexes behave as d-p-hybridized two-band materials in general, the pop complexes are well describable within d_{z^2}-single-band Hamiltonians [15]. Since the site-off-diagonal electron-phonon coupling is of little significance with the CDW backgrounds of the Fig. 1 type, we set α equal to zero. The rest of parameters are, unless otherwise noted, taken as $U_M = 1.2$, $V_{MXM} = 0.3$, and $\beta = 0.7$ for MX chains [1,32,33], while $U_M = 1.0$, $V_{MM} = 0.5$, $V_{MXM} = 0.3$, and $\beta = 1.4$ for MMX chains [19,26].

III. CALCULATIONAL PROCEDURE

We treat the Hamiltonians (1) within the Hartree-Fock approximation. The lattice distortion is adiabatically determined and can therefore be expressed in terms of the electronic density matrices $\langle n_{\mu:n,s}\rangle_{HF}$, where $\langle\cdots\rangle_{HF}$ denotes the thermal average over the Hartree-Fock eigenstates. Since no spontaneous deformation of the metal sublattice has been observed in any MX and MMX pop

complexes, we enforce the constraint $l_{n+1}^{(-)} + l_n^{(+)} = 0$ on every $M-X-M$ bond. Then the force equilibrium conditions

$$\frac{\partial\langle\mathcal{H}_{MX}\rangle_{HF}}{\partial l_n^{(\pm)}} = 0, \quad \frac{\partial\langle\mathcal{H}_{MMX}\rangle_{HF}}{\partial l_n^{(\pm)}} = 0, \tag{6}$$

yield

$$
\begin{aligned}
2K_{MX}l_n^{(-)} &= \beta\sum_s(\langle n_{\mu:n,s}\rangle_{HF} - \langle n_{\nu:n-1,s}\rangle_{HF}), \\
2K_{MX}l_n^{(+)} &= \beta\sum_s(\langle n_{\nu:n,s}\rangle_{HF} - \langle n_{\mu:n+1,s}\rangle_{HF}),
\end{aligned}
\tag{7}
$$

where $\mu = \nu = 1$ for MX chains, while $\mu = 1$, $\nu = 2$ for MMX chains.

The real part of the optical conductivity is given by

$$\sigma(\omega) = \frac{\pi}{N\omega}\sum_{\epsilon,\epsilon'}f(\epsilon)[1 - f(\epsilon')]|\langle\epsilon'|\mathcal{J}|\epsilon\rangle|^2\delta(\epsilon' - \epsilon - \hbar\omega),$$
$$\tag{8}$$

where $f(\epsilon) = (e^{\epsilon/k_BT} + 1)^{-1}$ and $\langle\epsilon'|\mathcal{J}|\epsilon\rangle$ is the matrix element of the current density operator $\mathcal{J}$ between the eigenstates of energy ϵ and ϵ'. $\mathcal{J}$ is defined as

$$\mathcal{J}_{MX} = j_{MXM}^{(1,1)}, \quad \mathcal{J}_{MMX} = j_{MM}^{(1,2)} + j_{MXM}^{(1,2)}, \tag{9}$$

for MX and MMX chains, respectively, with

$$j_{MM}^{(\mu,\nu)} = \frac{ie}{\hbar}c_{MM}t_{MM}\sum_{n,s}(a_{\nu:n,s}^\dagger a_{\mu:n,s} - a_{\mu:n,s}^\dagger a_{\nu:n,s}), \tag{10}$$

$$j_{MXM}^{(\mu,\nu)} = \frac{ie}{\hbar}c_{MXM}\sum_{n,s}[t_{MXM} - \alpha(l_{n+1}^{(-)} + l_n^{(+)})]$$
$$\times(a_{\mu:n+1,s}^\dagger a_{\nu:n,s} - a_{\nu:n,s}^\dagger a_{\mu:n+1,s}), \tag{11}$$

where c_{MM} and c_{MXM} are the average $M-M$ and $M-X-M$ distances, respectively, and are set for $c_{MXM} = 2c_{MM}$ [34,35].

In order to elucidate the intrinsic excitation mechanism, solitons are calculated at a sufficiently low temperature without any assumption on their spatial configurations. Charged solitons (S^σ; $\sigma = \pm$) are obtained by setting the numbers of up- and down-spin electrons, N_+ and N_-, both equal to $(p - 1/2)N - \sigma/2$, while spin-s neutral solitons [S^{0s}; $s = \pm\frac{1}{2}$] with $N_\pm = (p-1/2)N \pm s$, where N, taken to be 401 in our calculation, is the number of unit cells and p is the number of metal sites in the unit cell.
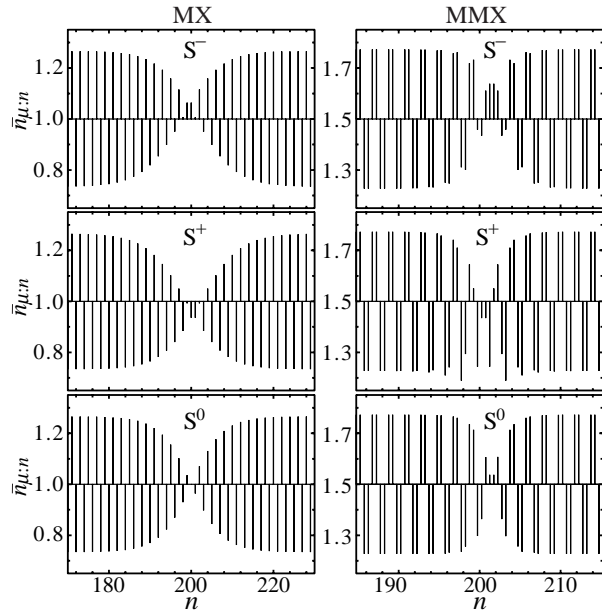
FIG. 2. Spatial configurations of the optimum solitons in MX and MMX chains.
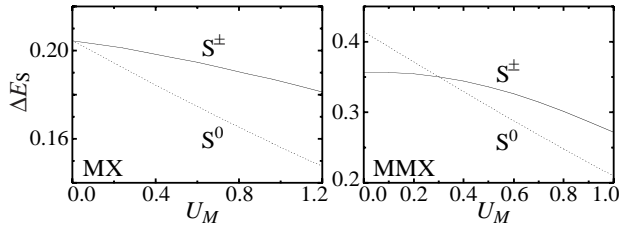

FIG. 3. The formation energies of the stably located solitons as functions of the Coulomb interaction, where $\beta = 0.7$ and U_M varies keeping the relation $U_M = V_{MXM}/0.25$ for MX chains, while $\beta = 1.4$ and U_M varies keeping the relation $U_M = V_{MM}/0.5 = V_{MXM}/0.3$ for MMX chains.

IV. RESULTS

We show the spatial configurations of the optimum solitons in Fig. 2 and plot their formation energies ΔE_S in Fig. 3. In MX chains, charged solitons are stable laying their centers on halogen sites, while neutral solitons on metal sites. In MMX chains, all the optimum solitons are halogen-centered. As the Peierls gap E_{gap} increases, solitons generally possess increasing energies and decreasing extents, and end up with immobile defects. U_M and V_{MM} reduce E_{gap} and thus enhance the mobility of solitons, while V_{MXM} has an opposite effect. Without any Coulomb interaction, the soliton formation energies are all degenerate and scaled by the Peierls gap as $\Delta E_S = E_{gap}/\pi$ in the weak-coupling region $E_{gap} \lesssim t_{MXM}$ [36], whereas their degeneracy is lifted and neutral solitons have higher energies than charged solitons with further increasing gap. Since E_{gap} decreases with increasing U_M, ΔE_S is a decreasing function of U_M. Neutral soli-

tons are more sensitive to the Coulomb interaction and thus their formation energy turns smaller than that of charged solitons with increasing U_M. Considering that E_{gap} is a linear function of U_M, we learn that neutral solitons well keep the scaling relation $\Delta E_S \propto E_{gap}$ against the Coulomb interaction.

Figure 2 suggests that an MX soliton of charge σ and spin s, $S^{\sigma s}$, described in terms of electrons is equivalent to its counterpart $S^{-\sigma -s}$ described in terms of holes. Such a symmetry is more directly observed through the energy structures shown in Fig. 4. Solitons generally exhibit an additional level within the gap. There appear further soliton-related levels in the strong-coupling region [37].
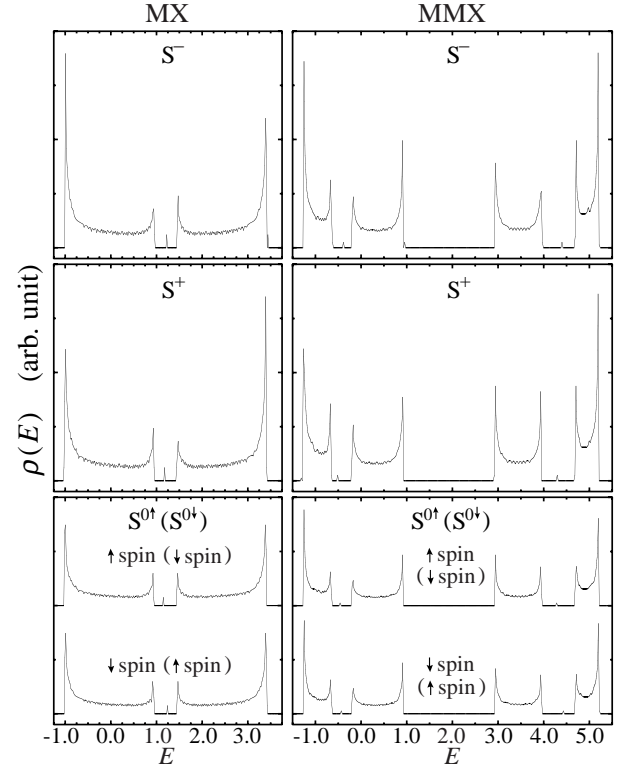

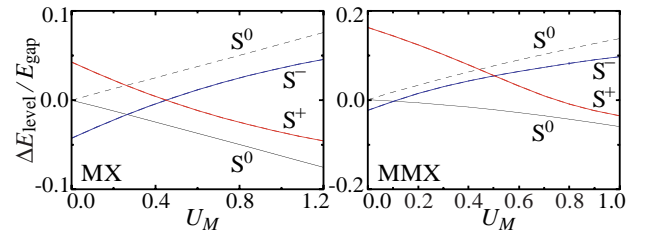FIG. 4. Density of states for the optimum soliton solutions.

FIG. 5. (Color online) Energy shifts of the localized soliton levels from the gap center scaled by the Peierls gap as functions of the Coulomb interaction. The parametrization is the same as that in Fig. 3. The level structures of up- and down-spin electrons are plotted by solid (broken) and broken (solid) lines, respectively, for $S^{0\uparrow}$ ($S^{0\downarrow}$), while they are degenerate for charged solitons.
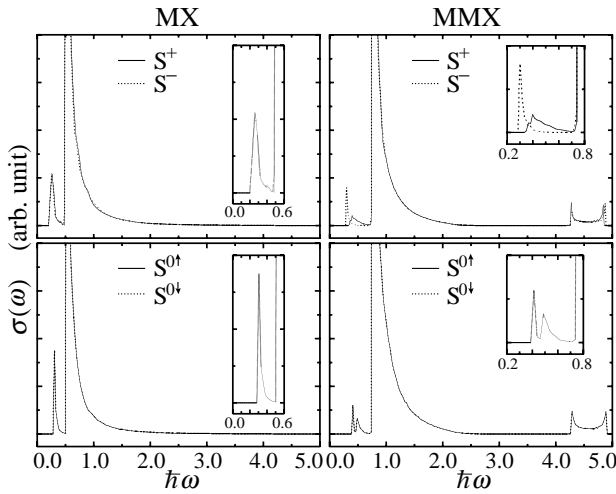
FIG. 6. Absorption spectra with a soliton excited for *MX* and *MMX* chains. The low-frequency structures are scaled up in insets.

The intragap soliton levels are analyzed in more detail in Fig. 5. When the coupling strength increases without any Coulomb interaction, the mid-gap level due to a neutral soliton keeps still, while the charged-soliton levels deviate from the gap center. symmetry. Once the Coulomb interaction is switched on, the neutral-soliton level also begins to move away from the gap center breaking the spin up-down Soliton-related electron and hole levels are necessarily symmetric with respect to the center of the gap in *MX* chains, while such a symmetry is generally broken in *MMX* chains. The electron-hole symmetry is kept and broken in the *MX* Hamiltonian (1a) and the *MMX* Hamiltonian (1b), respectively.

Now we show in Figure 6 photoinduced absorption spectra which are expected of *MX* and *MMX* chains. Since photoinduced solitons are necessarily in pairs, we superpose the S^- ($S^{0\downarrow}$) spectrum on the S^+ ($S^{0\uparrow}$) spectrum. The spectra of S^+ and S^- are degenerate for *MX* chains but distinguishable for *MMX* chains. *The asymmetry between the $S^\pm$ absorption bands can remain even in the absence of the Coulomb correlation provided the electron-phonon interaction is sufficiently strong.* Although the spectra of $S^{0\uparrow}$ and $S^{0\downarrow}$ are degenerate for both *MX* and *MMX* chains, those for *MMX* chains are interesting in themselves. The S^0 spectrum is single-peaked for *MX* chains but splits into two definite peaks for *MMX* chains. *The doublet structure of the S^0 spectrum is due to the combination of the broken electron-hole symmetry and relevant Coulomb correlation.* In principle *MX* chains also lose the electron-hole symmetry with their X p_z electrons activated [38], which indeed applies to the NiX compounds [39]. However, it is not the case with the PtX and PdX compounds, where the energy level of the X p_z orbitals is much lower than that of the M d_{z^2} orbitals and thus the p-orbital contribution may effectively be incorporated into the intermetal supertransfer energy of the single-band Hamiltonian (1a). In fact a two-band

calculation of the PtCl compound [40] still results in a single-peaked S^0 absorption band near the gap center.

V. SUMMARY AND DISCUSSION

Since polarons are generated only from electron-hole pairs with large excess energies, lower-energy-excited charge transfer excitons relax into soliton pairs or decay by luminescence [2]. A neutral-soliton pair has a lower formation energy [1,22,33,41] but a shorter life time [2] under realistic parametrizations. Photoexcited $[Pt(en)_2X](ClO_4)_2$ ($X = Cl, Br$) [42,43] and $[Pt(en)_2I](ClO_4)_2$ [44] indeed yield intragap absorptions attributable to neutral and charged solitons, respectively. The charged-soliton spectrum has a single-peaked Gaussian shape, which is well consistent with Fig. 6, while the neutral-soliton spectrum consists of a midgap main band and an accompanying shoulder structure, which demands further driving forces such as lattice fluctuations [32].

Solitons may be photogenerated in *MMX* complexes as well, yielding a contrastive absorption spectrum of doublet structure. The separation between the two S^0 bands is in proportion to the on-site Coulomb repulsion and may therefore be reduced with pressure applied, whereas the asymmetry between the two $S^\pm$ bands is sensitive to the electron-lattice coupling and may thus be enhanced by the halogen replacement $Cl \rightarrow Br \rightarrow I$. Photoinduced absorption measurements on *MMX* complexes may not only reveal the novel doublet structures of soliton-induced spectra but also give a key to the unsettled problem in *MX* complexes−the shoulder structure of the S^0 absorption spectrum. Let us make a close collaboration between experimental and theoretical investigations of dynamic properties of *MMX* complexes.

[1] J. T. Gammel, A. Saxena, I. Batistić, A. R. Bishop, and S. R. Phillpot, Phys. Rev. B **45**, 6408 (1992).

[2] H. Okamoto and M. Yamashita, Bull. Chem. Soc. Jpn. **71**, 2023 (1998).

[3] K. Nasu, J. Phys. Soc. Jpn. **52**, 3865 (1983).

[4] I. Batistić, J. T. Gammel, and A. R. Bishop, Phys. Rev. B **44**, 13228 (1991); H. Röder, A. R. Bishop, and J. T. Gammel, Phys. Rev. Lett. **70**, 3498 (1993).

[5] H. Okamoto, T. Mitani, K. Toriumi, and M. Yamashita, Mater. Sci. Eng. B **13**, L9 (1992).

[6] J. T. Gammel and G. S. Kanner, Synth. Met. **70**, 1191 (1995).

[7] W. P. Su, J. R. Schrieffer, and A. J. Heeger, Phys. Rev. Lett. **42**, 1698 (1979); Phys. Rev. B **22**, 2099 (1980).

[8] H. Takayama, Y. R. Lin-Liu, and K. Maki, Phys. Rev. B **21**, 2388 (1980).

[9] S. Ichinose: Solid State Commun. **50** (1984) 137.

[10] Y. Onodera: J. Phys. Soc. Jpn. **56** (1987) 250.

[11] D. Baeriswyl and A. R. Bishop, J. Phys. C **21**, 339 (1988).

[12] N. Kuroda, M. Sakai, Y. Nishina, M. Tanaka, and S. Kurita, Phys. Rev. Lett. **58**, 2122 (1987).

[13] H. Okamoto, T. Mitani, K. Toriumi and, M. Yamashita, Phys. Rev. Lett. **69**, 2248 (1992).

[14] M. Kuwabara and K. Yonemitsu, Mol. Cryst. Liq. Cryst. **341**, 533 (2000); **343**, 47 (2000); J. Phys. Chem. Solids **62**, 435 (2001).

[15] S. Yamamoto, Phys. Lett. A **258**, 183 (1999); J. Phys. Soc. Jpn. **69**, 13 (2000); Phys. Rev. B **63**, 125124 (2001).

[16] H. Kitagawa, N. Onodera, T. Sonoyama, M. Yamamoto, T. Fukawa, T. Mitani, M. Seto, and Y. Maeda, J. Am. Chem. Soc. **121**, 10068 (1999).

[17] S. Yamamoto, J. Phys. Soc. Jpn. **70**, 1198 (2001).

[18] B. I. Swanson, M. A. Stroud, S. D. Conradson and M. H. Zietlow, Solid State Commun. **65**, 1405 (1988); M. A. Stroud, H. G. Drickamer, M. H. Zietlow, H. B. Gray, and B. I. Swanson, J. Am. Chem. Soc. **111**, 66 (1989).

[19] S. Yamamoto, Phys. Rev. B **64**, 140102(R) (2001).

[20] H. Matsuzaki, T. Matsuoka, H. Kishida, K. Takizawa, H. Miyasaka, K. Sugiura, M. Yamashita, and H. Okamoto, Phys. Rev. Lett. **90**, 046401 (2003).

[21] H. Kitagawa, N. Onodera, J.-S. Ahn, and T. Mitani, Synth. Met. **86**, 1931 (1997).

[22] S. Yamamoto and M. Ichioka, J. Phys. Soc. Jpn. **71**, 189 (2002); S. Yamamoto, Mol. Cryst. Liq. Cryst. **379**, 555 (2002).

[23] S. Jin, T. Ito, K. Toriumi, and M. Yamashita, Acta Cryst. C **45**, 1415 (1989).

[24] N. Kimura, H. Ohki, R. Ikeda, M. Yamashita, Chem. Phys. Lett. **220**, 40 (1994).

[25] Y. Wada, T. Furuta, M. Yamashita, and K Toriumi, Synth. Met. **70**, 1195 (1995).

[26] M. Kuwabara and K. Yonemitsu, J. Mater. Chem. **11**, 2163 (2001).

[27] L. G. Butler, M. H. Zietlow, C.-M. Che, W. P. Schaefer, S. Sridhar, P. J. Grunthaner, B. I. Swanson, R. J. H. Clark, and H. B. Gray, J. Am. Chem. Soc. **110**, 1155 (1988).

[28] S. A. Borshch, K. Prassides, V. Robert, and A. O. Solonenko, J. Chem. Phys. **109**, 4562 (1998).

[29] C. Bellitto, A. Flamini, L. Gastaldi, and L. Scaramuzza, Inorg. Chem. **22**, 444 (1983).

[30] C. Bellitto, G. Dessy, and V. Fares, Inorg. Chem. **24**, 2815 (1985).

[31] S. Yamamoto, Phys. Lett. A **247**, 422 (1998); Synth. Met. **103**, 2683 (1999).

[32] K. Iwano and K. Nasu, J. Phys. Soc. Jpn. **61**, 1380 (1992).

[33] Y. Tagawa and N. Suzuki, J. Phys. Soc. Jpn. **64**, 2212 (1995).

[34] C.-M. Che, F. H. Herbstein, W. P. Schaefer, R. E. Marsh, and H. B. Gray, J. Am. Chem. Soc. **105**, 4604 (1983).

[35] R. J. H. Clark, M. Kurmoo, H. M. Dawes, and M. B. Hursthouse, Inorg. Chem. **25**, 409 (1986).

[36] S. Yamamoto, Phys. Rev. B **66**, 165113 (2002).

[37] Y. Tagawa and N. Suzuki, J. Phys. Soc. Jpn. **59**, 4074 (1990).

[38] J. T. Gammel, R. J. Donohoe, A. R. Bishop, and B. I. Swanson, Phys. Rev. B **42**, 10566 (1990).

[39] H. Okamoto, Y. Shimada, Y. Oka, A. Chainani, T. Takahashi, H. Kitagawa, T. Mitani, K. Toriumi, K. Inoue, T. Manabe, and M. Yamashita, Phys. Rev. B **54**, 8438 (1996).

[40] S. W. Weber-Milbrodt, J. T. Gammel, A. R. Bishop, and E. Y. Loh, Jr., Phys. Rev. B **45**, 6435 (1992).

[41] K. Iwano, J. Phys. Soc. Jpn. **66**, 1088 (1997).

[42] N. Kuroda, M. Ito, Y. Nishina, and M. Yamashita, J. Phys. Soc. Jpn. **62**, 2237 (1993).

[43] H. Okamoto, Y. Kaga, Y. Shimada, Y. Oka, Y. Iwasa, T. Mitani, and M. Yamashita, Phys. Rev. Lett. **80**, 861 (1998).

[44] H. Okamoto, Y. Oka, T. Mitani, and M. Yamashita, Phys. Rev. B **55**, 6330 (1997).